Journal of Digital Imaging (2018) 31:505–512
https://doi.org/10.1007/s10278-018-0051-5

Development and Validation of Segmentation Method for Lung Cancer Volumetry on Chest CT

Young Jae Kim[1,2] · Seung Hyun Lee[2] · Kun Young Lim[3] · Kwang Gi Kim[1]

Published online: 29 January 2018
© Society for Imaging Informatics in Medicine 2018

Abstract
The set of criteria called Response Evaluation Criteria In Solid Tumors (RECIST) is used to evaluate the remedial effects of lung cancer, whereby the size of a lesion can be measured in one dimension (diameter). Volumetric evaluation is desirable for estimating the size of a lesion accurately, but there are several constraints and limitations to calculating the volume in clinical trials. In this study, we developed a method to detect lesions automatically, with minimal intervention by the user, and calculate their volume. Our proposed method, called a spherical region-growing method (SPRG), uses segmentation that starts from a seed point set by the user. SPRG is a modification of an existing region-growing method that is based on a sphere instead of pixels. The SPRG method detects lesions while preventing leakage to neighboring tissues, because the sphere is grown, i.e., neighboring voxels are added, only when all the voxels meet the required conditions. In this study, two radiologists segmented lung tumors using a manual method and the proposed method, and the results of both methods were compared. The proposed method showed a high sensitivity of 81.68–84.81% and a high dice similarity coefficient (DSC) of 0.86–0.88 compared with the manual method. In addition, the SPRG intraclass correlation coefficient (ICC) was 0.998 (CI 0.997–0.999, $p < 0.01$), showing that the SPRG method is highly reliable. If our proposed method is used for segmentation and volumetric measurement of lesions, then objective and accurate results and shorter data analysis time are possible.

Keywords Lung cancer · Response evaluation criteria in solid tumors · Tumor volume · Computed tomography · Computer-assisted diagnosis

Introduction

Lung cancer has the highest incidence and mortality rates among cancer cases worldwide. In the USA, the survival rate was only 17% from 2003 to 2009 and the mortality rate was 29.5% for men and 26.1% for women from 2006 to 2010 [1]. For this reason, clinical categorization, proper treatment, and objective response assessment of cancer cases are required [2, 3]. The Response Evaluation Criteria In Solid Tumors (RECIST), published by an international collaboration of the European Organization for Research and Treatment of Cancer (EORTC) and the National Cancer Institute of the USA, is used in clinical fields for the objective assessment of treatment effects. RECIST categorizes lesions with the longest diameter ≥ 10 mm as measured by a spiral computed tomography (CT) scan as measurable lesions. Up to five of these measurable lesions are identified as target lesions, and the sum of the longest diameter of these target lesions is used as the reference on which to evaluate the response to treatment [4]. However, a one-dimensional (1D) diameter does not reflect the real size of a lesion. To accurately calculate the size of a lesion and evaluate small changes, volumetric evaluation is necessary. Zhao et al. [5] found that volumetric measurement is more sensitive in detecting changes in a lesion than existing 1D measurements. However, all three-dimensional (3D) boundaries must be defined to measure the volume of a lesion, but defining the boundaries is time-

Kun Young Lim and Kwang Gi Kim contributed equally to this work.

✉ Kwang Gi Kim
kimkg@gachon.ac.kr

[1] Department of Biomedical Engineering, Gachon University College of Medicine, 21, Namdong-daero 774 beon-gil, Namdong-gu, Incheon 21565, Republic of Korea

[2] Department of Plazma Bio Display, Kwangwoon University, 20 Kwangwoon-ro, Nowon-gu, Seoul 01897, Republic of Korea

[3] Department of Diagnostic Radiology, Center for Lung Cancer, National Cancer Center, 323 Ilsan-ro, Ilsandong-gu, Goyang 10408, Gyeonggi-do, Republic of Korea

consuming and difficult. In addition, interrater variability makes manual measurement less reliable.

Our study aimed to resolve the problems of the manual measurement of a lesion by developing a semiautomatic 3D tumor segmentation method based on computer-aided diagnosis (CAD) to compute the volume of a tumor. CAD is an ancillary diagnostic tool with various image-processing techniques for performing difficult measurements. Physicians save time with CAD because tumor volume is measured almost automatically using a variety of indices such as intensity or relationship between pixels [6, 7]. Additionally, the objective and quantitative measurements yield results with high reproducibility and reliability. In a comparison of manual volumetric measurement and automatic volumetric measurement using CAD to evaluate tumor response to chemotherapy, Marten [8] showed that there was no significant mismatch among the radiologists with the automatic measurement, but the manual measurement had a 24% mismatch among the radiologists. Currently, most studies in which CAD was used focused on isolated lung cancer; published studies on lung cancer with involvement of the chest wall or mediastinum are rare. In addition, the accuracy of the results of studies on lung cancer with involvement of the chest wall or mediastinum is generally low because the unclear boundary between tumor tissue and normal tissue makes segmentation difficult. In 2013, Gu et al. [9] designed a 3D region-growing algorithm using a lung tumor analysis (LuTA) application with CT images to perform automatic lung cancer segmentation and obtained an average similarity of 78.01% with 15 manual measurements. In 2014, Guo et al. [10] used automatic segmentation of tumors via a Markov random field model in positron emission tomography/computed tomography (PET/CT) and obtained a dice similarity coefficient (DSC) of 0.85 ± 0.013 for seven CT scans. Also in 2014, Cui et al. [11] used automatic segmentation via a graph-based model in PET/CT and obtained a DSC of only 0.791 for 20 CT scans. Of the abovementioned studies, the Guo et al. study was the only one that showed relatively high accuracy. However, it required the use of PET and CT together and only two-dimensional (2D) segmentation was possible. In addition, the number of scans used (seven) was not sufficient to obtain reliable results. The main purpose for using CAD for tumor segmentation in lung cancer cases is to minimize manual intervention. However, the segmentation results of some tumors that have invaded the chest wall or mediastinum require modification by some manual intervention because of low accuracy. In addition, using CAD for only isolated tumors is inefficient. To overcome these limitations, we propose and verify an algorithm that accurately segments lung cancer of various types such as isolated cancers or invaded cancers with minimal user intervention.

Materials and Methods

Study Dataset and Development Environment

For our study, we collected CT images of the chest from 80 patients (49 men, 31 women; age range = 43–79 years) receiving chemotherapy at the Korean National Cancer Center and periodically assessed the images using the RECIST guidelines. CT images were 512 × 512 pixels and in 16-bit Digital Imaging and Communications in Medicine (DICOM) format. Information about each patient was deleted, and all CT data were classified and managed using serial numbers. Programs used in the experiment were Microsoft Visual Studio (ver. 2010, Microsoft Corp., Redmond, WA, USA), ITK (Insight Segmentation and Registration Toolkit; Kitware Inc., Clifton Park, NY, USA), and VTK (Visualization Toolkit; Kitware Inc.).

Manual Segmentation

To assess the accuracy of the proposed segmentation method, we used the results of manual segmentation as the gold standard. Using software developed in-house, the tumor was outlined manually to define the region of interest (ROI). The ROI was drawn on all axial planes where the tumor was present, and all ROIs were joined to construct the 3D model.

Semiautomatic Segmentation

The proposed method begins with the user setting the seed point at the center of the tumor and performing a preprocessing step before conducting the algorithm following the flowchart shown in Fig. 1.

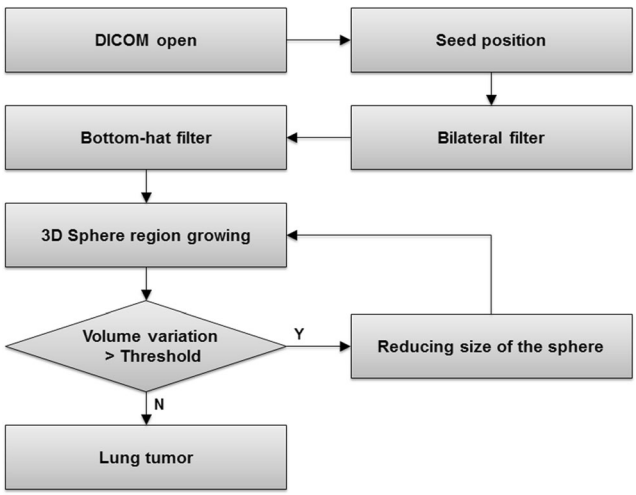

Fig. 1 Flowchart of the proposed algorithm

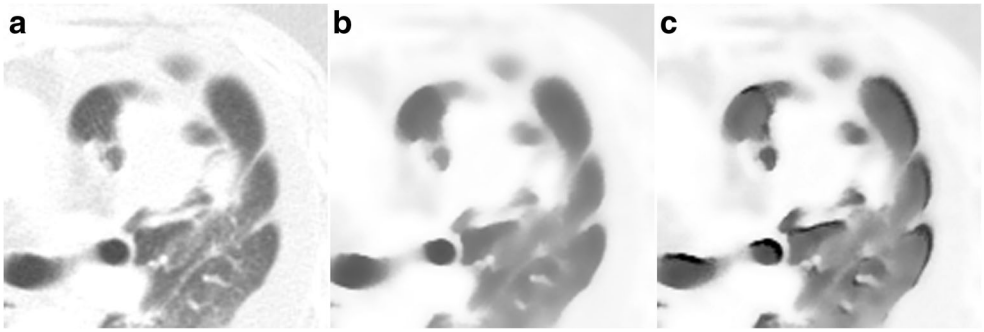

Fig. 2 Result of image improvement. **a** Original image. **b** Result of denoising by using a bilateral filter. **c** Improved image after using a bottom-hat filter

Preprocessing

Preprocessing was conducted to reduce image noise and improve image quality and thus increase the accuracy of lesion segmentation. A bilateral filter was used to denoise the image because of the difficulty in using an anisotropic diffusion filter. The filter reduces noise using a smoothing and range parameter while preserving the edge of the image effectively [12]. Figure 2b shows that the noise was entirely removed, but the edge of the lesion was hardly effected despite decreasing the noise.

After denoising, the image underwent improvement to help in the accurate classification of surrounding tissues. The goal of image improvement is the clear segmentation of the lesion by increasing the pixel gradient and adjusting the image contrast. The bottom-hat filter is used to emphasize the bright side and darken the other side of an image [13]. We maximized the contrast between tumor and tissues by combining the bottom-hat-filtered image and the original image (Fig. 2c).

Tumor Segmentation

The 3D region-growing algorithm was used to detect the tumor. Region growing is a general method for segmenting a homogeneous region by expanding out from a seed point in 3D. The expansion of the region is efficient when the target area is clearly separate from the surrounding area [14–16]. However, leakage occurs when a pixel does not satisfy the region-growing criterion. When the tumor has invaded the chest wall or mediastinum in the CT image, the general region-growing algorithm has a risk of leakage due to the similar contrast distribution between the tumor and the surrounding tissues. Accordingly, we developed the spherical region-growing (SPRG) method in which a 3D spherical mask is used to prevent leakage from neighboring tissues. Figure 3 shows the concept of the SPRG algorithm. A collection of voxels, W, on a segmented region undergoing analysis is defined as

$$W = \{(x,y,z) \notin \mathrm{RG} | N(x,y,z) \cap \mathrm{RG} \neq \varnothing\}, \quad (1)$$

where $N(x, y, z)$ are 26 neighboring voxels to voxel (x, y, z) in W, and RG is a collection of voxels detected in this iteration. W consists of surrounding voxels that have not yet been checked. All voxels in W are determined suitable for inclusion in RG by checking the growing condition, which is defined by Eqs. 2 and 3:

$$\delta_1(x,y,z,\mathrm{RG}) = \mathrm{mean}(\mathrm{RG}) - 2\mathrm{SD}(\mathrm{RG}), \quad (2)$$

$$\delta_2(x,y,z,\mathrm{RG}) = \mathrm{mean}(\mathrm{RG}) + 2\mathrm{SD}(\mathrm{RG}). \quad (3)$$

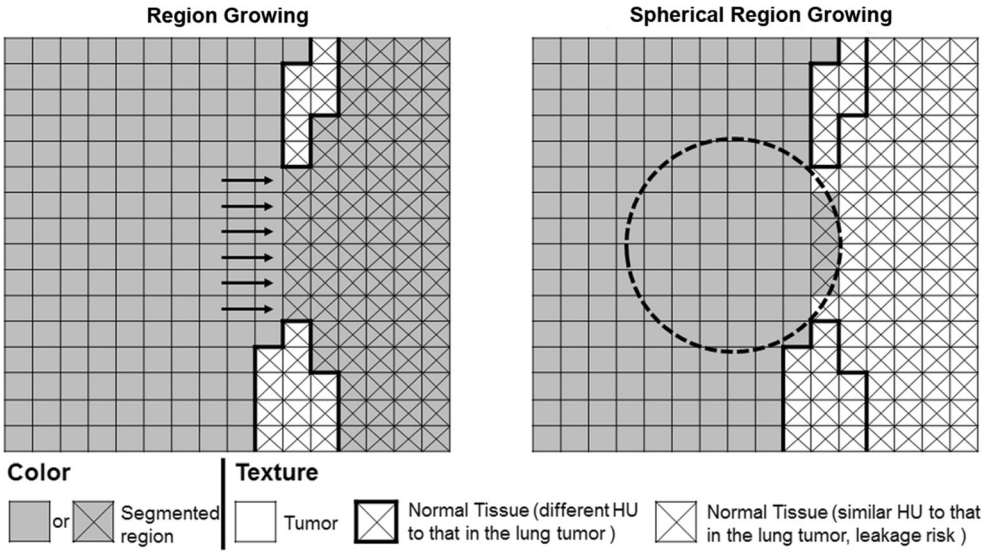

Fig. 3 Comparison of the concept of general region-growing algorithms and that of the proposed algorithm

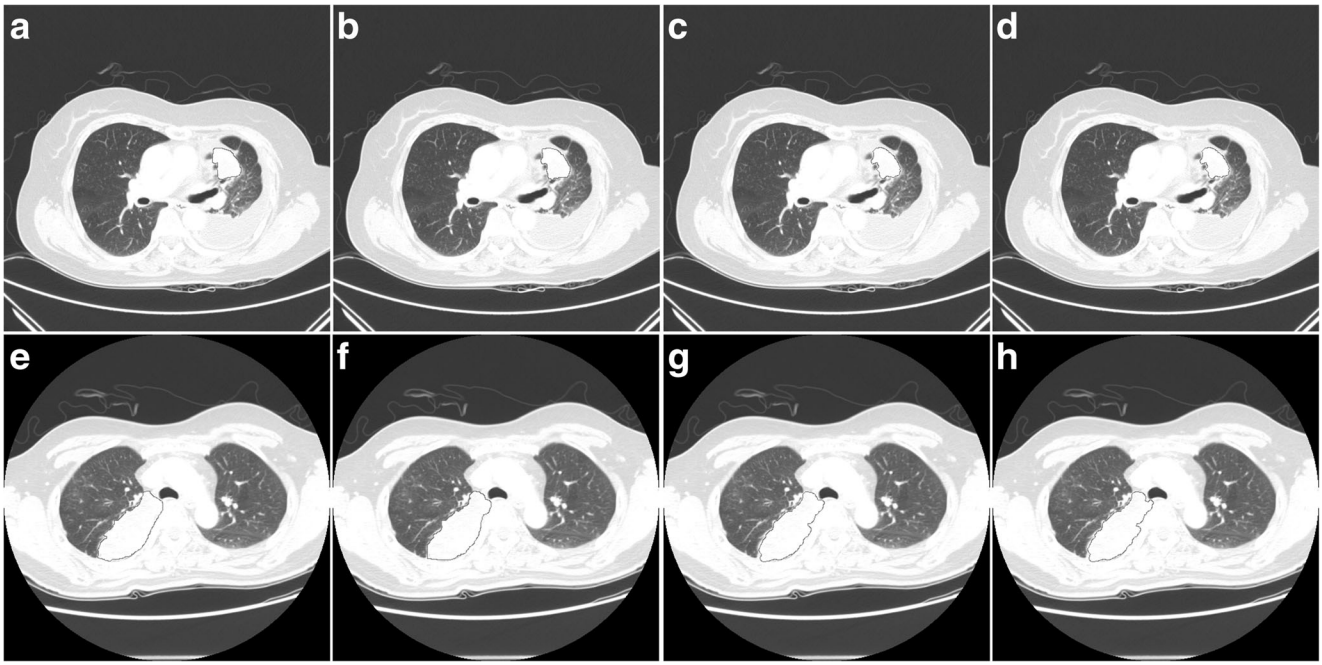

Fig. 4 Comparison of the segmentation results between the manual and the SPRG. **a**, **e** Results of the Manual1. **b**, **f** Results of the Manual2. **c**, **g** Results of the SPRG1. **d**, **h** Results of the SPRG2

Because RG voxels are added to every growth region, the growing condition changes by adapting to the brightness distribution of the tumor as the region is grown.

In a general region-growing method, the growing condition around the current voxel (x, y, z) is examined. However, in our method, inspection occurs around $\delta_1(x, y, z, \mathrm{RG})$ and $\delta_2(x, y, z, \mathrm{RG})$ using a 3D spherical mask $S(x, y, z)$ defined as

$$S(x,y,z) = \left\{ (x_i, y_i, z_i) | (x_i - x)^2 + (y_i - y)^2 + (z_i - z)^2 \leq r^2 \right\}, \tag{4}$$

$$C(x,y,z) = \left\{ \left(x_j, y_j, z_j\right) | \left(x_j, y_j, z_j\right) \in S(x,y,z) \wedge \left(x_j, y_j, z_j\right) : \delta_1(x,y,z,\mathrm{RG}) \leq g\left(x_j, y_j, z_j\right) \leq \delta_2(x,y,z,\mathrm{RG}) \right\}, \tag{5}$$

where $S(x, y, z)$ is a set of voxels (x_i, y_i, z_i) in a 3D sphere of radius r and centered at current voxel (x, y, z). $C(x, y, z)$ is the set of voxels around $S(x, y, z)$ that satisfy the growing condition of $\delta_1(x, y, z, \mathrm{RG})$ and $\delta_2(x, y, z, \mathrm{RG})$. All voxels in $C(x, y, z)$ are elements of $S(x, y, z)$, and $g(x_j, y_j, z_j)$ is the brightness of each voxel (x_j, y_j, z_j) in a set of voxels in the range of $\delta_1(x, y, z, \mathrm{RG})$ and $\delta_2(x, y, z, \mathrm{RG})$.

After the examination of growth conditions is completed, the current voxel (x, y, z) is checked for inclusion in RG using Eq. 6:

$$\theta[S(x,y,z), C(x,y,z)] = \begin{cases} 1, & \text{if } S(x,y,z) - C(x,y,z) = \varnothing \\ 0, & \text{otherwise} \end{cases} \tag{6}$$

Table 1 Comparison of sensitivity, specificity, accuracy, and DSC between the results of the manual and the SPRG measurements

		Sensitivity (%)	Specificity (%)	Accuracy (%)	DSC
Manual1	SPRG1	81.68	99.97	99.89	0.86
	SPRG2	81.69	99.97	99.89	0.86
Manual2	SPRG1	84.81	99.97	99.91	0.88
	SPRG2	84.73	99.97	99.91	0.87

Table 2 Verification and comparison of the results of the SPRG and the manual volumetric measurements

	Mean ± standard deviation	*F*	*P* value[a]	ICC	*P* value[b]
Manual1	45.39 ± 60.83	0.161	0.922	0.998	< 0.01
Manual2	44.37 ± 59.19				
SPRG1	40.48 ± 54.58				
SPRG2	40.48 ± 54.55				

[a] *P* value for ANOVA test

[b] *P* value for ICC

If $S(x, y, z)$ and $C(x, y, z)$ are the same, then all voxels in the 3D sphere have met the growing condition. Thus, $\theta[S(x, y, z), C(x, y, z)] = 1$ and RG includes the current voxel (x, y, z).

In the proposed method, if the leakage area is smaller than the 3D sphere of radius r, the tumor is segmented and leakage is prevented. However, if the leakage area is greater than the 3D sphere of radius r, leakage occurs. Therefore, the appropriate size of the 3D sphere must be determined. The size of the 3D sphere is determined automatically as it changes according to the change in the volume resulting from segmentation.

Results

We segmented a lung tumor on a chest CT image using our 3D SPRG method. The result is shown in Fig. 4.

We also compared and performed statistical analysis on the results of manual segmentation and segmentation using the proposed SPRG method for 80 cases. The two radiologists who participated in the study detected the lung tumor in the same 80 cases via manual measurement (Manual1, Manual2). In addition, they performed lung tumor segmentation using the SPRG method (SPRG1, SPRG2). The volume of the tumor was determined based on all of the detected results.

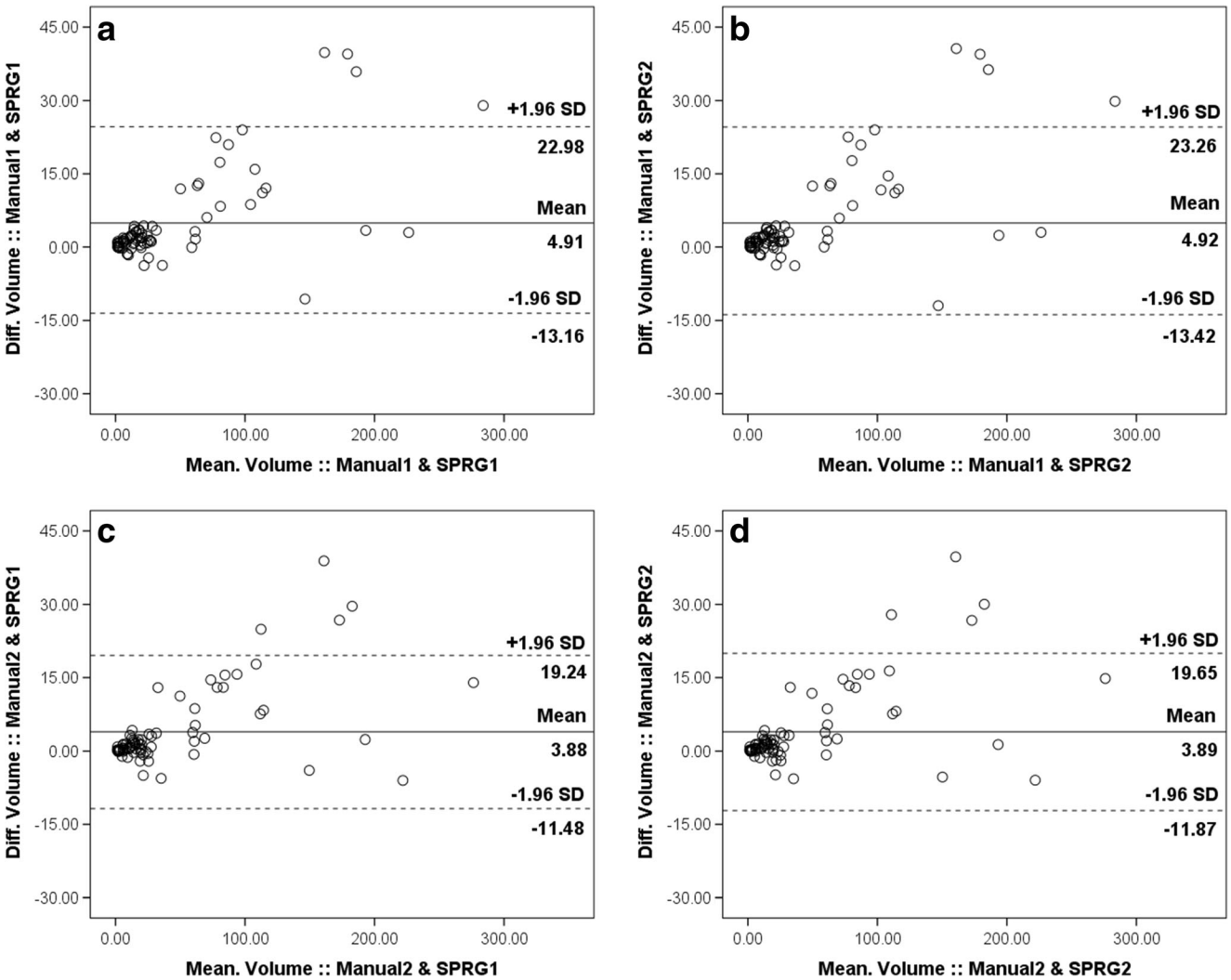

Fig. 5 Bland–Altman plots comparing the manual and the SPRG volumetric measurements. **a** Manual1 and SPRG1. **b** Manual1 and SPRG2. **c** Manual2 and SPRG1. **d** Manual2 and SPRG2

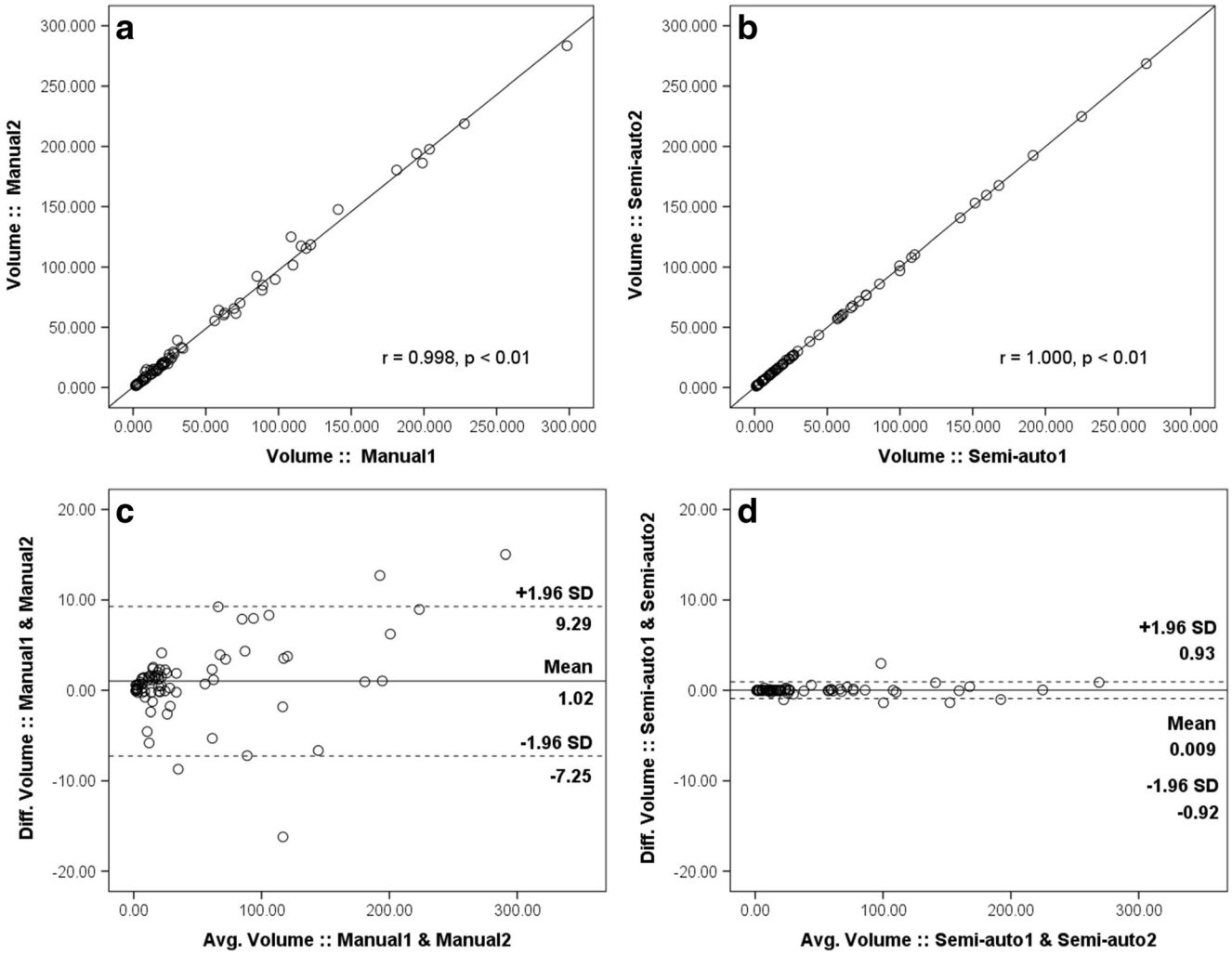

Fig. 6 Interobserver variation of the measured volume. **a** Scatter plot comparing the Manual1 and the Manual2. **b** Scatter plot comparing the SPRG1 and the SPRG2. **c** Bland–Altman plot comparing the Manual1 and the Manual2. **d** Bland–Altman plot comparing the SPRG1 and the SPRG2

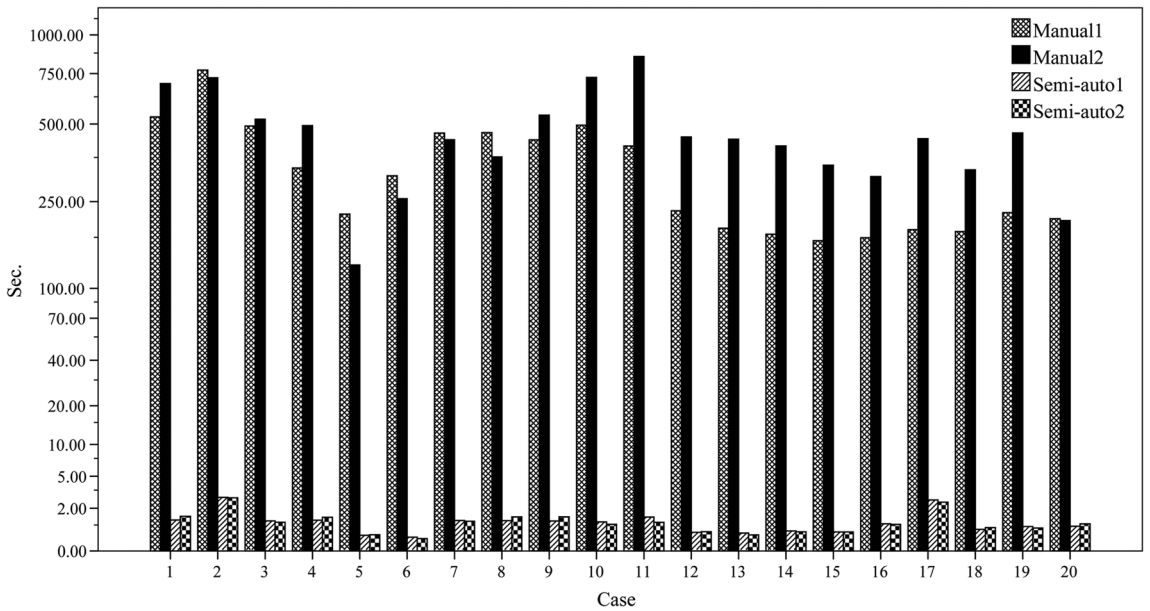

Fig. 7 Comparison of elapsed time needed for segmentation of 20–40-ml tumor

The accuracy of the SPRG measurement method was evaluated using sensitivity, specificity, accuracy, and DSC. For evaluation, we obtained true positive (TP), false positive (FP), true negative (TN), and false negative (FN) by calculating, pixel-by-pixel, the position of the lung tumor detected by the SPRG and manual methods; the results are presented in Table 1. The sensitivity of SPRG1 and SPRG2 compared to that of Manual1 was 81.68 and 81.69%, respectively, and the DSC was 0.86 for both. The sensitivity of SPRG1 and SPRG2 compared to that of Manual2 was 84.81 and 84.73%, respectively, and the DSC was 0.88 and 0.87.

We also evaluated the comparability, correlation, and reliability of the results of the manual and SPRG volumetric measurements using comparative analyses. In addition, the clinical reliability of the measured volume obtained using the SPRG method was verified on the basis of the results of the comparative analyses. We performed a one-way ANOVA test, obtained Bland–Altman plots for the equivalence of the measurement results, and determined the intraclass correlation coefficient (ICC) for reliability.

The mean volume determined by Manual1 and Manual2 was 45.39 ± 60.83 and 44.37 ± 59.19 ml, respectively. On the other hand, the mean volume determined by SPRG1 and SPRG2 was 40.48 ± 54.58 and 40.48 ± 54.55 ml, respectively. The median volume of Manual1 and Manual2 was 19.88 ml (quartile 8.35, 62.84) and 18.84 ml (quartile 7.78, 61.72), respectively, and that of SPRG1 and SPRG2 was 18.39 ml (quartile 7.34, 7.14) and 18.39 ml (quartile 7.14, 58.54), respectively. There is significant correlation between the two SPRG volumes and Manual1: SPRG1 $r = 0.993$, $p < 0.01$; SPRG2 $r = 0.993$, $p < 0.01$. Besides, the volumes of SPRG1 and SPRG2 show significant correlation with the volume of Manual2.

The one-way ANOVA test result for the volumes determined by the manual and SPRG measurements, presented in Table 2, shows no significant differences between the two methods ($F = 0.161$, $p > 0.05$). The ICC for the manual and SPRG volumetric measurements indicates a reliability as high as 0.998 (CI 0.997–0.999, $p < 0.01$). In the Bland–Altman plots, the bias between the manual method and the SPRG method measured by the two radiologists was in the range 3.88–4.92 ml, and the variability between each graph was constant (Fig. 5).

The interobserver variation between and the segmentation time of the manual and the SPRG measurement methods were compared to verify the clinical usefulness of the proposed method. To compare the error, interobserver correlation analysis was performed and Bland–Altman plots were created, as shown in Fig. 6. Although the manual measurement had a high interobserver correlation ($r = 0.998$, $p < 0.01$) (Fig. 6a), that of the SPRG measurement was even higher ($r = 1.000$, $p < 0.01$) (Fig. 6b). Bland–Altman plots confirmed that the interobserver difference of the volume measured by the SPRG method (Fig. 6d) is less than that of volume measured by the manual method (Fig. 6c).

To evaluate the usefulness of the SPRG method, we selected 20 CT scans, out of the 80, that had a 20–40-ml tumor and compared the elapsed time before a lung tumor was detected by the SPRG method and the manual method. The mean elapsed time of Manual1 and Manual2 was 335.21 ± 165.69 and 458.63 ± 182.87 s, respectively, and that of SPRG1 and SPRG2 was only 1.14 ± 0.62 and 1.15 ± 0.61 s, respectively (Fig. 7).

Discussion

The RECIST guideline, widely used to objectively evaluate the treatment response of lung tumors, is based on the diameter, not the volume, of the tumor. Because measuring the volume of a tumor is difficult and time-consuming, the use of RECIST in clinics is difficult. Thus, we proposed the SPRG method for the segmentation and measurement of lung tumors using computer image-processing techniques. The sensitivity of the result of SPRG segmentation compared to that of the results of the manual method used by two radiologists (Manual1 and Manual2) was 81.68–84.81% with a DSC of 0.86–0.88. This result is more accurate than the results of other studies that attempted autosegmentation of lung tumors (Table 3). In addition, the high accuracy of the SPRG method was confirmed using 80 CT scans, while the majority of other studies used fewer than 20 CT scans. Three main factors contributed to this positive result: use of a 3D region-growing

Table 3 Comparison of the semiautomatic segmentation of lung tumors by our proposed method with that of other studies that used semiautomatic segmentation

	Modality	Algorithm	Case	Validity
Yuhua Gu et al.	CT	Multi 3D region growing	15	SI 78.29(vs Reader1)
				SI 77.72 (vs Reader2)
Guo Yu et al.	PET/CT	Markov random field model	7	DSC 0.85 ± 0.013
Cui Hui et al.	PET/CT	Graph-based model	20	DSC 0.791
Proposed method	CT	SPRG	80	DSC 0.873 (vs Reader1)
				DSC 0.891 (vs Reader2)

method instead of a probability distribution-based algorithm to detect a lung tumor with various shapes, inclusion of as much potential area with a lung tumor as possible by using a localized adaptive region-growing method, and the minimization of error extension by using a 3D sphere in the image.

The ANOVA test and the ICC result presented in Table 2 show the clinical reliability of the proposed method. The ANOVA test results showed no significant difference between the manual and SPRG volumetric measurements, and the ICC (0.99) for the manual and SPRG volumetric measurements indicated high reliability for the SPRG method.

The interobserver variation between the manual and SPRG measurement methods is shown in Fig. 6. The segmentation results of the SPRG method indicated that they had a higher interobserver correlation than those of the manual method. In addition, the Bland–Altman plots showed that the interobserver difference of the volume measured by the SPRG method was less than that of the volume measured by the manual method. Therefore, the SPRG method has the potential for providing more objective results and results with better reproducibility than the manual method.

Comparison of elapsed time for segmentation by the two methods showed an approximately 347-fold reduction in time needed for tumor detection by the SPRG method. The manual method required ~ 6 min to detect a 30-ml lung tumor, while the SPRG method needed only 1 s. It is expected that the bigger the lung tumor, the more significant the time reduction.

The proposed method does not always achieve complete segmentation of lung tumors. In some cases, there is an ~ 20% error between the results from the proposed method and those of the radiologist that requires post-processing manual modification. Nevertheless, segmenting lung tumors with the proposed method and making a minor correction is more effective than performing the entire lung tumor segmentation manually.

A CT image is the basic element of our proposed method, but the proposed algorithm was designed by considering the relative values of pixels and morphological characteristics. Because the algorithm is simple and easy to use, it can be applied to other lesions such as brain and breast tumors and can work with other medical imaging techniques such as MRI.

Finally, significant reduction in procedure time and quantitative as well as objective results can be achieved with our proposed method for the segmentation and volumetric measurement of a lung tumor. Additionally, the method can be a supplement to RECIST in the evaluation of the response to treatment. The proposed method has the potential for evaluating the response to treatment more accurately and objectively.

Funding Information This work was supported by a grant from the National Cancer Center (1410570-2), Gachon University (GCU 2017-0211), and Ministry of Trade, Industry and Energy, Republic of Korea (10079501)

Compliance with Ethical Standards

This retrospective study was approved by the Institutional Review Board (IRB) of National Cancer Center of Korea with waiver of the requirement for patients' informed consent (NCC2014-0199).

Conflict of Interest The authors declare that they have no conflict of interest.

References

1. Siegel R, Ma J, Zou Z, Jemal A: Cancer statistics, 2014. CA Cancer J Clin 64:9–29, 2014
2. Osterlind K: Chemotherapy in small cell lung cancer. Eur Respir J 18:1026–1043, 2001
3. Thatcher N, Ranson M, Lee SM, Niven R, Anderson H: Chemotherapy for non-small cell lung cancer. Ann Oncol 6:S83–S95, 2000
4. Eisenhauer EA, Therasse P, Bogaerts J, Schwartz LH, Sargent D, Ford R, Dancey J, Arbuck S, Gwyther S, Mooney M, Rubinstein L, Shankar L, Dodd L, Kaplan R, Lacombe D, Verweij J: New response evaluation criteria in solid tumours: revised RECIST guideline (version 1.1). Eur J Cancer 45:228–247, 2009
5. Zhao B, Schwartz L, Moskowitz C: Lung cancer: computerized quantification of tumor response—Initial results 1. Radiology 241:892–898, 2006
6. Doi K: Computer-aided diagnosis in medical imaging: historical review, current status and future potential. Comput Med Imaging Graph 31:198–211, 2007
7. van Ginneken B, Schaefer-Prokop CM, Prokop M: Computer-aided diagnosis: how to move from the laboratory to the clinic. Radiology 261:719–732, 2011
8. Marten K, Auer F, Schmidt S, Kohl G, Rummeny E, Engelke C: Inadequacy of manual measurements compared to automated CT volumetry in assessment of treatment response of pulmonary metastases using RECIST criteria. Eur Radiol 16:781–790, 2006
9. Gu Y, Kumar V, Hall LO, Goldgof DB, Li C-Y, Korn R, Bendtsen C, Velazquez ER, Dekker A, Aerts H, Lambin P, Li X, Tian J, Gatenby RA, Gillies RJ: Automated delineation of lung tumors from CT images using a single click ensemble segmentation approach. Pattern Recognit 46:692–702, 2013
10. Guo Y, Feng Y, Sun J, Zhang N, Lin W, Sa Y, Wang P: Automatic lung tumor segmentation on PET/CT images using fuzzy Markov random field model. Comput Math Methods Med 401201:2014, 2014
11. Cui H, Wang X, Zhou J, Fulham M, Eberl S, Feng D: Topology constraint graph-based model for non-small-cell lung tumor segmentation from PET volumes. In: International Symposium on Biomedical Imaging (ISBI), 2014 I.E. 11th. pp. 1243–1246, 2014
12. Elad M: On the origin of the bilateral filter and ways to improve it. IEEE Trans Image Process 11:1141–1151, 2002
13. Das S, Mohan A: Medical image enhancement techniques by bottom hat and median filtering. Int J Electron Commun Comput Eng 5:347–351, 2014
14. Adams R, Bischof L: Seeded region growing. IEEE Trans Pattern Anal Mach Intell 16:641–647, 1994
15. R. Pohle and K. D. Toennies: Segmentation of medical images using adaptive region growing. In: SPIE 4322, Medical Imaging 2001. 1337–1346, 2001
16. Revol-Muller C, Peyrin F, Carrillon Y, Odet C: Automated 3D region growing algorithm based on an assessment function. Pattern Recognit Lett 23:137–150, 2002